Defects and external field effects on the electronic properties of a carbon nanotube torus

A. Latgé,[1,*] C. G. Rocha,[1] L. A. L. Wanderley,[1] M. Pacheco,[2] P. Orellana,[3] and Z. Barticevic[4]
[1]*Instituto de Física, Universidade Federal Fluminense, 24210-340 Niterói-RJ, Brazil*
[2]*Departamento de Física, Universidad de Santiago de Chile, Chile*
[3]*Departamento de Física, Universidad Católica do Norte, Antofogasta, Chile*
[4]*Departamento de Física, Universidad Técnica F. Santa Maria, Casilla 110-V, Valparaiso, Chile*
(Received 4 October 2002; published 29 April 2003)

Electronic properties of toroidal carbon nanotubes are studied adopting a single π-band tight binding Hamiltonian and following real-space renormalization techniques within the Green function formalism. The analysis is restricted to the achiral torus and the dependence of the toroidal energy spectra on its radius and thickness (tube radius) is inferred from the local density of states. The possibility of a metal-insulating transition occurrence in infinite single tubes and toroidal is investigated as functions of magnetic and electric fields applied in distinct configurations. As expected, periodical Aharonov-Bohm oscillations in the local density of states at the Fermi level of the nanostructures are found as a result of the annular symmetry. When substitutional impurities are taken into account such an oscillatory behavior is found to be preserved. Effects of vacancy defects on the electronic properties are also discussed.

DOI: 10.1103/PhysRevB.67.155413 PACS number(s): 73.63.Fg, 73.22.−f

I. INTRODUCTION

Transmission electron microscopy data[1] reported recently suggest an experimental evidence of a peculiar circular formation of carbon nanotubes (CN's) called toroidal carbon nanotubes (TCN's). Metal catalytic particles are supposed to act as a kind of plug, linking both edges of the structure during the growing process. Perfect carbon coils, stabilized only by van der Waals forces were reported by Martel *et al.*[2] A torus obtained by bending around a single nanotube and connecting its two ends, forming a so called toroidal polyhex[3] was theoretically considered by Meumier *et al.*[4] They have found that the minimum torus radius allowed by elasticity conditions is of the order of 1500 Å, which agrees with the value found experimentally. Toroidal nanostructures made of a single carbon nanotube may be described as long rolled graphite sheets bent around in the form of tori, satisfying simultaneously transversal and longitudinal periodical boundary conditions.

Due to the particular geometries and sizes of CN's and TCN's, the study of fundamental phenomena in quantum physics such as the Aharonov-Bohm (AB) effect is a natural task. Magnetoconductance measurements on CN's, considering magnetic field applied in the axial direction,[5,6] have clearly indicated the presence of well-known periodic AB oscillations. Electronic properties of CN's were investigated theoretically considering magnetic-field configurations parallel and perpendicular to the nanotube axis.[7,8] In toroidal nanotubes, the AB pattern is expected for a magnetic field threading the torus plane and has been discussed by Haddon.[9] It is hence of interest to perform a comparative study between the effects of magnetic fields applied through these more intricated nanostructured systems (TCN's) and on perfect infinite CN's.

For the sake of simplicity we restrict our analysis to zigzag/armchair (Z/A) and armchair/zigzag (A/Z) torus. Here we present a detailed theoretical study of the correlation between geometric aspects of the toroidal systems and their corresponding electronic properties (semiconducting or metallic). Additionally, we also discuss the effects of defects such as vacancies and impurities on the electronic properties, modeled here via a quite simple approximation. Our general model calculation, entirely defined on a real-space Hamiltonian, has been shown to be very appropriate for the description of nanotube heterojunctions,[10] multiwalled systems,[11] and quantum dot structures based on CN's.[12,13]

The presence of a homogeneous magnetic field threading the annular system is described within the Peierls-phase approximation.[8,14] The effects of an electric field, also applied perpendicularly to the torus plane, on the electronic properties is analyzed within the same picture and we discuss the possibilities of the survival of the AB oscillations. We believe that a better understanding of the physics of TCN's, even within such a simple picture as the one adopted here, should help us to propose their utilization in real nanodevices. The experimental evidence reported recently of nanojunctions formations[15] after high electric fields applications on multiwalled nanotube arrays is just one of the numerous examples of experimental realizations based on these particular carbon tubes.

II. LOCAL ELECTRONIC PROPERTIES

The studied achiral TCN's are defined as $(n,n,N,0)$ for (A/Z) and $(n,0,N,N)$ for (Z/A), following the standard notation of the a CN chiral vector $\mathbf{C}=(n,m)$; n, m, and N being integer numbers. The energy dispersion relation of a toroidal structure is easily obtained from the tight-binding graphene relation by imposing periodic boundary conditions, leading to the quantization rules for both k components.[16–18]

Rather than using the k-space picture, we treat the Hamiltonian of the TCN entirely in real space and consider a loop of connected rings described within a single π-band tight-binding approximation. One should remark that the adopted

single-orbital tight-binding treatment restrict our results to an energy range close to the Fermi level. The torus radius depends on the number of rings used to close the system as follows. For an A/Z torus it is equal to $R=aN/(2\pi)$, whereas for the Z/A configuration $R=a\sqrt{3}N/4\pi$, N being the number of rings and a the graphene lattice parameter (2.46 Å). One should notice that for a zigzag (armchair) CN configuration $(n,0)$ $[(n,n)]$, a ring comprises $2n$ $(4n)$ carbon atoms disposed in two atomic sublayers along the circumferential tube direction. By adopting an iterative process one is able to solve a set of coupled matricial Dyson equations for the local Green functions and then define a generation rule for the TCN in which the undressed locator (diagonal Green function) and hopping matrices suffer a sequence of renormalization steps whose number of iterations defines the torus radii. The energy spectra is then obtained from the energy position of the peaks of the local electronic density of states (LDOS). The LDOS of a TCN composed of j rings may be obtained directly from the imaginary part of the corresponding renormalized diagonal Green function,[10–13] as

$$\rho_0^j(\omega)=-\frac{1}{n'\pi}\mathrm{Img}\{\mathrm{tr}[\tilde{G}_{0,0}^j(\omega)]\}, \tag{1}$$

n' being the number of carbon atoms in a single ring.

For a Z/A torus configuration, we have

$$\tilde{G}_{0,0}^j(\omega)=[\tilde{1}-\tilde{g}^j(\tilde{V}_1+\tilde{V}_2^{*j})\tilde{g}^{*j}(\tilde{V}_1+\tilde{V}_2^j)]^{-1}\tilde{g}^j, \tag{2}$$

with $\tilde{g}^j(\omega)$, $\tilde{g}^{*j}(\omega)$, $\tilde{V}_2^{*j}$, and $\tilde{V}_2^{*j}$ being dressed Green functions and hopping matrices which may be written in terms of the corresponding quantities associated with a torus composed of $j-2$ rings as

$$\tilde{g}^j=[\tilde{1}-\tilde{A}_2^{j-2}\tilde{V}_2^{j-2}\tilde{g}_0^{*j-2}\tilde{V}_1\tilde{A}_1^{j-2}\tilde{V}_1\tilde{g}_0^{*j-2}\tilde{V}_2^{j-2}]^{-1}\tilde{A}_2^{j-2}, \tag{3}$$

$$\tilde{g}^{*j}=[\tilde{1}-\tilde{g}_0\tilde{V}_2\tilde{A}_1^{j-2}\tilde{V}_2]^{-1}\tilde{g}_0, \tag{4}$$

and

$$\tilde{V}_2^{*j}=\tilde{V}_2^{*j-2}\tilde{g}^{*j-2}\tilde{V}_1\tilde{A}_1^{j-2}\tilde{V}_2,$$

$$\tilde{V}_2^j=\tilde{V}_2\tilde{A}_1^{j-2}\tilde{V}_1\tilde{g}^{*j-2}\tilde{V}_2^{*j-2}, \tag{5}$$

where

$$\tilde{A}_2^n=[\tilde{1}-\tilde{g}^n\tilde{V}_2^{*n}\tilde{g}^{*n}\tilde{V}_2^n]^{-1}\tilde{g}^n,$$

$$\tilde{A}_1^n=[\tilde{1}-\tilde{g}_0\tilde{V}_1\tilde{g}^{*n}\tilde{V}_1]^{-1}\tilde{g}_0, \tag{6}$$

where $\tilde{V}_1$ and $\tilde{V}_2$ are the undressed hopping matrices used in a CN zigzag tight-binding description and $g_0=1/(\omega-E_0)$ is the undressed locator.[10] Similar recursion equations may be written for an A/Z TCN. One of the advantages of working within such a real-space framework is that all the microscopic details of the nanostructure are naturally taken into account. This allows one, in addition, to include different types of defects.

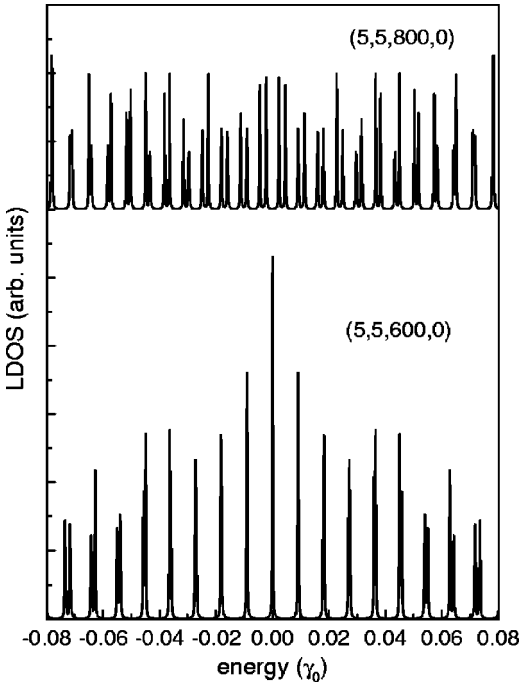

FIG. 1. Local density of states as a function of energy for (5,5,800,0) and (5,5,600,0) TCN's. Energies are written in terms of the hopping integral between nearest neighbors: ≈ 3 eV.

Results for the density of states of armchair/zigzag TCN's $(5,5,N,0)$ are shown in Fig. 1 for two values of N. Within the adopted one-band scheme the energies are usually written in terms of the hopping element $V_{\pi,\pi}=\gamma_0$ which is of the order of 3 eV.[14] Both the LDOS's exhibit a sequence of discrete electronic states[16] reflecting the intrinsic finite size of the closed loop. One may also notice that the number of rings (N) dictates the existence of a state at the Fermi level $(E_F=0)$. For our calculations we call a system a metal if it has an occupied state at the Fermi level. In that sense, for a metallic armchair CN closed in a torus with a number of rings that is a multiple of 3 (metallic zigzag configuration in the transverse torus direction) one may have a metalliclike TCN. This is quite an interesting result related to the particular correspondence between topology and electronic properties of infinite tubes[19,20] and which are also reflected in the annular structure discussed in the present work. The quantization rules for A/Z TCN's, leads to sampling of the translational wave vector component in units of $2\pi/na$. As the band structures of armchair tubes exhibit two bands crossing the Fermi energy at $k=2\pi/3a$, one clearly concludes that only for N a multiple of 3 is it possible to obtain an eigenstate at the Fermi level. Similar results were also obtained for finite armchair nanotubes[21] in a detailed investigation of the transmission through finite parts of CN's, using tight binding Hamiltonians and adopting both single- and double-band models.

This kind of feature is also shown in Fig. 2(a), where the explicitly dependence of the energy spectra (states next to the Fermi level) on the torus radius (given here by N) is displayed. For all considered A/Z TCN's, a discrete state appears at the Fermi level provided $N=3m$, as a reminis-

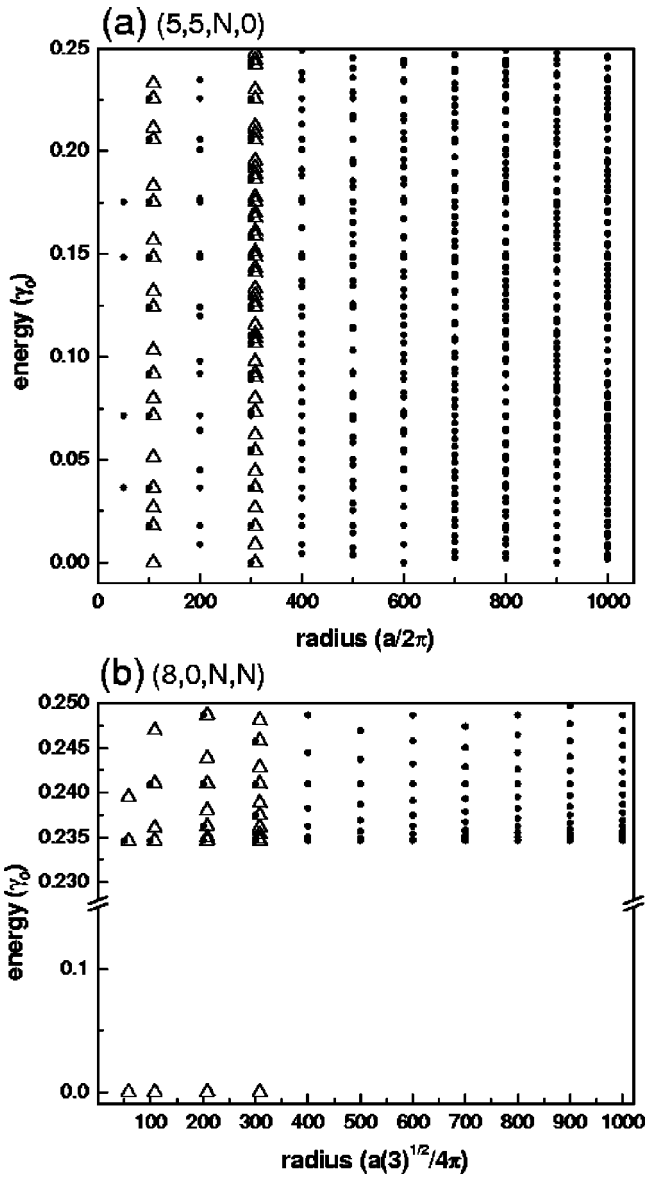

FIG. 2. Dependence of the energy spectra on the torus radius for (a) (5,5,*N*,0) and (b) (8,0,*N*,*N*) TCN's. The radius *R* are written in terms of the lattice parameter *a*. Up triangles denote energy spectra with a vacancy for some radius values.

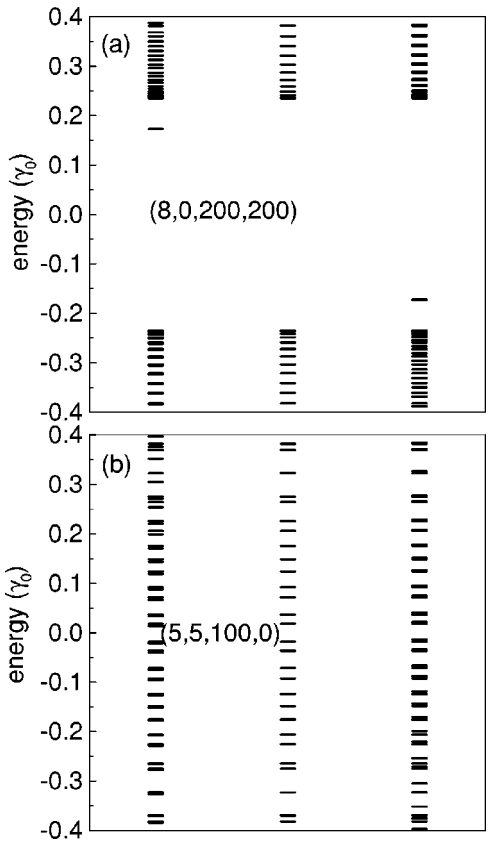

FIG. 3. Energy spectra considering a substitutional impurity on a random site of a (a) (8,0,200,200) TCN and a (b) (5,5,100,0) torus. The right (left) set of levels corresponds to a donorlike (acceptor) impurity whereas the central columns are the results for the pure case.

cence of the metallic character of the corresponding zigzag CN. Otherwise, for a *Z*/*A* structure with a semiconducting zigzag configuration [see Fig. 2(b)], the toroidal gap is essentially given by the nanotube radius and does not depend on the torus radius (R). As expected, for increasing N values, spectra corresponding to perfect infinite CN's are achieved.

Also shown in Fig. 2 are the results corresponding to the energy spectra of both types of TCN's in which a vacancy is created by just removing one atom at a random site[23] of the structure. For both TCN's (*A*/*Z* and *Z*/*A*) the presence of a vacancy clearly lifts the degeneracy of the states, splitting each one of the discrete states into two. For all values of N, a localized state appears at the Fermi level resembling the results obtained for a graphene sheet with vacancies whose local density of states exhibits a well-defined peak at and near the Fermi level.[22]

An example of the effects of a substitutional impurity on TCN energy spectra is displayed in Fig. 3 for (8,0,200,200) and (5,5,200,0) TCN's. Similar to what occurs in traditional semiconducting materials, acceptorlike or donorlike states also appear next to the valence or conduction bands, respectively. As expected, the corresponding binding energies depend on the rates between host and impurity diagonal energies in the tight binding Hamiltonian. For both ''disordered'' *A*/*Z* and *Z*/*A* TCN's, one notices again the split of the discrete levels into two new states. Of course, a detailed analysis of such impurity effects must go beyond the single π-band tight binding description presented.

For instance, the conductance of infinite CN's presenting vacancies or substitutional impurities was also calculated following the Landauer formalism. Our transport results indicated that the hydrogenic-impurity case is qualitatively well described within this simple theory (to be published). However, in the case of vacancies one must carefully incorporate other σ orbitals to correctly predict the energy positions at which the conductance, due to backscattering mechanisms, suffers a reduction predicted by *ab initio* calculations.[24]

III. EXTERNAL FIELD EFFECTS ON THE ENERGY SPECTRA

A. Magnetic field

Different groups[5–8] have studied before the main changes produced in the electronic structure of infinite CNs due to the presence of a magnetic field. It was shown that the gap size of a CN may be periodically modulated by increasing the magnetic flux threading the tube in the axial direction; the modulation period being determined by its electronic characteristic at zero field. Here we discuss how external fields modify the electronic properties of torus nanotubes and the role played by the geometric details on the changes.

To include magnetic field effects (applied perpendicularly to the torus plane) we adopt the Peierls approximation[8,14,25] in which a phase is essentially added to the hopping integrals of the tight binding Hamiltonian. Of course, the phase depends on the spatial atomic configuration of the tubes and also on the chosen potential-vector gauge. Within the effective mass framework[7,17,18] it was shown that the wave vector k changes to $k+\phi/R\phi_0$ in the presence of a magnetic field, ϕ being the magnetic flux enclosed by the torus, usually written in terms of the flux quantum ($\phi_0=hc/e$). Based on the Green function formalism we have obtained similar results for the dependence of the density of states and the gap energies on the magnetic flux, as those previously reported by Lin *et al.*[17,18]

Results for the density of states of some TCN's as a function of the energy and its dependence on the magnetic flux are illustrated in Fig. 4. The discrete nature of the TCN states, due to its finite size, is evident in Fig. 4(a) in which the LDOS is given by a sequence of well defined peaks, shifted in the presence of an axial magnetic field. The explicit dependence of the energy spectra on the magnetic flux corresponding to the metallic (9,0,200,200) and a semiconducting (8,0,200,200) TCN structures is shown in Figs. 4(b) and 4(c), respectively. The gap evolution of the metallic (9,0,200,200) TCN under a magnetic flux [see Fig. 4(b)] is essentially the same of the one corresponding to a metallic zigzag CN (9,0).[8] Otherwise, one may notice the quite weak influence of the flux intensity on the first state above the gap of the semiconducting Z/A TCN shown in Fig. 4(c); as the torus radius increases this magnetic field effect is evenly reduced. Contrarily, the higher states depend on the magnetic flux. Actually, this particular energy spectrum exhibits quite the same behavior as the one associated to a very narrow semiconductor quantum ring.[26,27] The increasing number of discrete states as the torus radius increases is shown in the spectra of Fig. 5(a) and 5(b), concerned with A/Z TCN's as well as the changing from ''metallic'' to semiconducting features depending on the N (torus radius) and flux values.[16,17]

The energy spectra pattern obtained for the case of a (9,0,100,100) torus with a substitutional impurity as a function of the magnetic flux is shown in Fig. 6 (up triangles). Although being a small TCN ($R=45$ Å) the main qualitative results would not be quite different for experimental (larger) torus. The results for a pure TCN are also displayed (solid circles) for comparison; the main difference being the split of each one of the latter discrete levels into two levels, one of them almost pinned at the previous energy position. These results indicate that the oscillatory dependence of the energy spectra on the magnetic flux (AB) is preserved against the lack of symmetry imposed by this kind of defect. Other defects such as the heptagon-pentagon pairs (topological defect) and quantum-dot formations along the annular structure may also be considered.

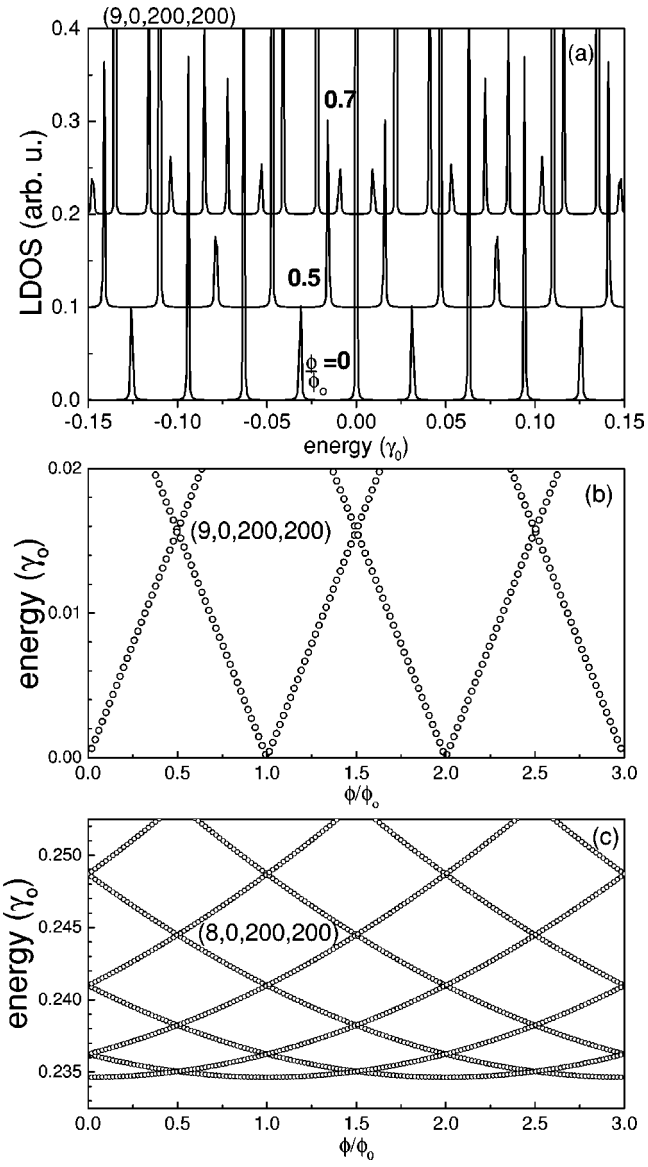

FIG. 4. (a) LDOS of a (9,0,200,200) TCN as a function of the energy for three values of the magnetic flux (0, 0.5, and 0.7) and dependence of the energy spectra on the magnetic flux for (b) (9,0,200,200) and (c) (8,0,200,200) TCN's.

We have also investigated, the limitations of the assumption of considering the vector potential at the toroid surface constant and equal to $\phi/2\pi R$. For very thin TCN's this is a good approach (and used up to now in all calculations). To take the nanotube thickness (r) into account one has to change it to $\phi/2\pi R[1-r/R\sin(x/r)]$, x being the atomic position along the nanotube circumferential direction. The analysis of the results for the energy changes of the first states (in relation to the zero energy) indicates, however, that

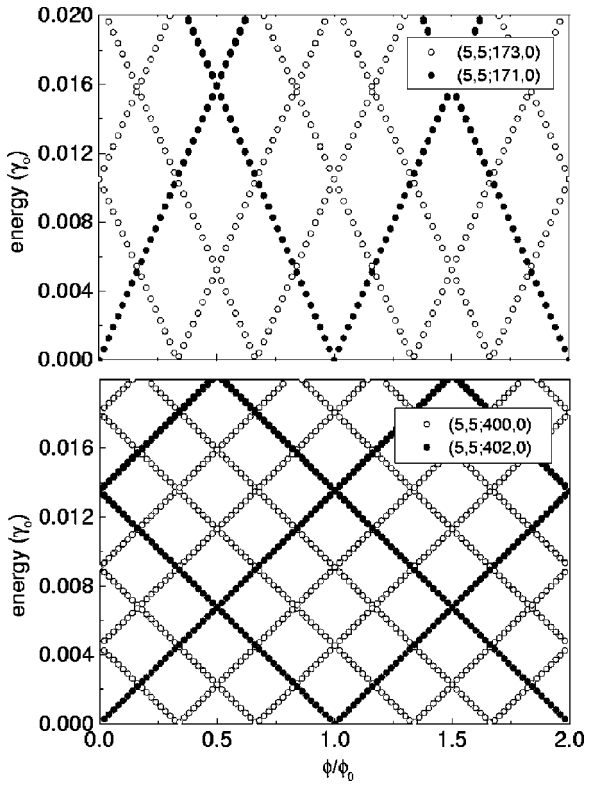

FIG. 5. Energy spectra of (5,5,N,0) TCN's as a function of the magnetic flux (a) $N=140$ and 141 and in (b) $N=400$ and 402.

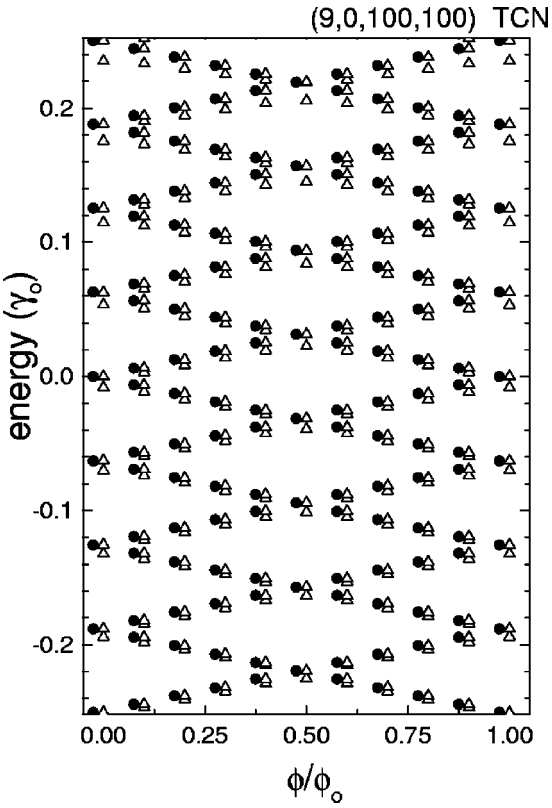

FIG. 6. Energy spectra for a (9,0,100,100) TCN as a function of the magnetic flux (full circles). Up triangles are the results for the same TCN with a substitutional impurity. The circles are shift in the x axis in order to better display the differences between both cases.

for TCN's composed of CN's with radii between 5 to 15 Å, the corrections are actually quite small and should be completely disregarded. Only for CN's with larger diameters (for which the rate r/R is not too small) should this magnetic effect play a relevant role. One should notice that CN's with larger radii than the usual ones are now available through new growth techniques.[28]

B. Electric field effects

Changes in the electronic spectra of both CN's and TCN's are now considered due to the presence of uniform transverse electric fields which may be viewed, for instance, as being generated by two capacitor planes displayed on and up the tubes.

Within the adopted tight-binding approximation, the effects of an electric field applied perpendicularly to the axis of an infinite CN is included in the on-site energies of carbon atoms in the Hamiltonian, following a linear interpolation for the potential energy difference along the nanotube diameter[29] (called in what follows the ''effective electric field energy,'' given in units of γ_0). Of course, this may take into account the microscopic details of the spatial distribution of the carbon atoms along the annular structures.

The dependence of the LDOS at the Fermi level on the electric field energy, for different values of magnetic flux (applied in the axial tube direction) is shown in Figs. 7(a) and 7(b) for a (9,0) CN and in Fig. 7(c) for a (10,0) tube. It is interesting to notice that the main features exhibited in the set of figures are quite similar to the behavior of the LDOS as a function of the energy: the same sequence of one-dimensional ''van Hove singularities'' typical of the quasi-one-dimensional CN's. One should remark that although we have extended our analysis to electric field energies up to $0.5\gamma_0$ (for the sake of illustration), actually, a quite smaller energy range can be experimentally proven[15] with variations depending upon the nanotube diameters.

The metal-insulator transition allowed by the application of an axial magnetic field depends now upon the electric-field energy value. An electronic transitionlike diagram is shown in Fig. 8 for three semiconducting zigzag CN's, illustrating the possible combination of magnetic and electric fields to allow the metal-insulator transition. As expected, the angular coefficients of the lines behave as r^{-1}, with r being the nanotube radius. This coupled effect of both applied electric and magnetic fields may be used in some devices to conveniently drive electronic transport.

Going to toroidal nanotubes, magnetic and electric fields are now considered in the direction perpendicular to the torus plane, i.e., the applied fields are both parallel to the torus axis. An expected result for that particular field configuration should be the splitting of the original discrete states (for zero electric field) into double ones as a consequence of the degeneracy lift of the nonequivalent carbon atoms of the unit cell. This effect and also the shift of the discrete states (to higher energies due to the electric field) are clearly shown in Fig. 9(a) which illustrates the results for the LDOS of a

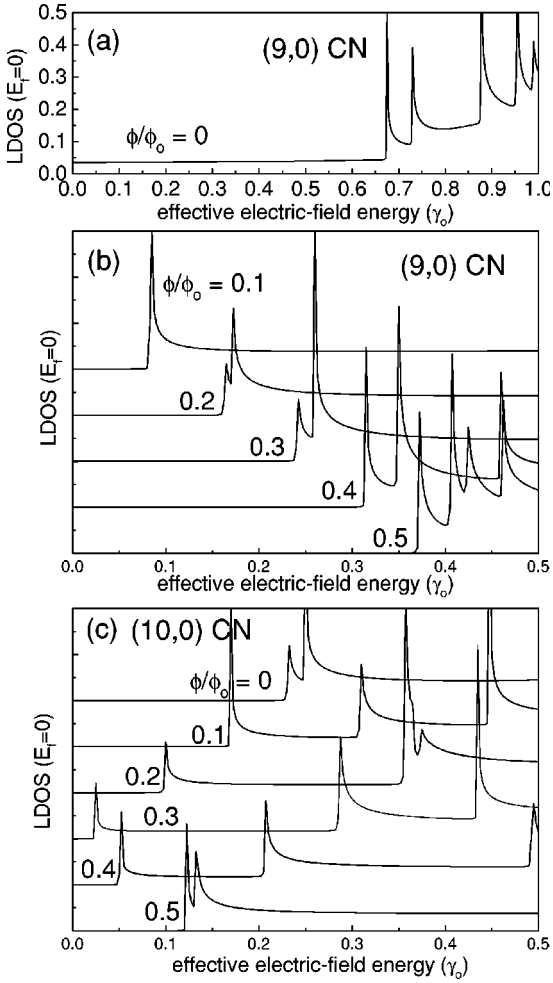

FIG. 7. Dependence of the LDOS at the Fermi level ($E_F=0$) on the effective electrical field for metallic [(a) and (b)] and semiconducting (c) zigzag CN's, for different magnetic flux.

(9,0,200,200) TCN, considering a magnetic flux equal to $0.5\phi_0$ and an effective electric field of $0.2\gamma_0$.

The quite complex dependence on both fields requires a more detailed analysis to point out the correct role played by each one individually. Figure 9(b) displays the dependence of the LDOS at the Fermi level for the same TCN, on the effective electric-field energy for two magnetic flux intensities, illustrating, once more, the complexity of the energy spectra.

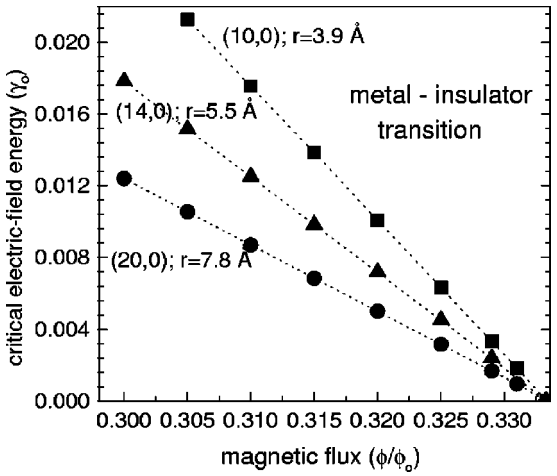

FIG. 8. Metal-insulator transition diagram as functions of the magnetic flux and the critical effective electric-field energy at $E_F=0$, for zigzag CN's of different radii (r).

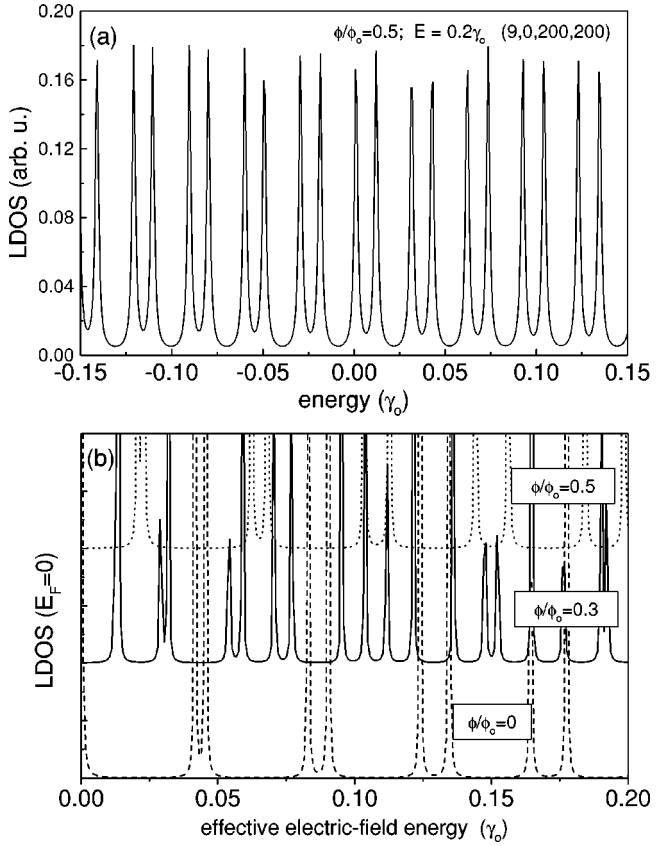

FIG. 9. LDOS as a function of the (a) energy and (b) effective electric field at the $E=0$ (both in terms of γ_0) for a (9,0,200,200) TCN. In (a) $\phi/\phi_0=0.5$ and $E=0.2\gamma_0$.

One should summarize saying that CN's and correlated structures (in particular the studied toroidal nanotubes) exhibit a variety of electronic properties depending upon their intrinsic geometric formation. Adding external fields, one may intentionally modify these properties and modulate their physical responses. Many of these physical configuration possibilities are easily handed within the real-space Hamiltonian and the renormalization techniques we have used to describe the TCN's in the present work. As they are intrinsically quasi-one-dimensional structures the quantum size manifestation appears naturally and one may, moreover, deal with interesting problems related to quantum interference phenomena. This is the case, for instance, of nanotube rings with two or four metallic contacts which may be idealized as composed of metallic nanotubes. Very recently, a new type of transistor made of nanotube rings was realized experimentally,[30] showing the possibility of nanometer-scale electronic circuits composed of nanotubes. Investigation on physical transport properties of ringlike systems is a natural extension and we are working along these lines.

ACKNOWLEDGMENTS

We would like to thank Drs. R. B. Muniz and M. F. dos Santos for useful discussions. This work was partially supported by the Brazilian Agencies CNPq, Fundação Vitae, and FAPERJ. M.P., P.O., and Z.B. would like to thank Fondecyt for support (Grant Nos. 1010429 and 7010429), CYTED, and the Millenium Scientific Nucleus (Grant No. ICM P99-135-F).

*Electronic address: latge@if.uff.br

[1] J. Liu, H. Dai, F. H. Halfner, D. T. Colbert, R. E. Smalley, S. J. Tans, and C. Dekker, Nature (London) **385**, 780 (1997).
[2] R. Martel, H. R. Shea, and P. Avouris, Science **398**, 299 (1999).
[3] E. C. Kirby, R. B. Mallion, and P. Pollak, J. Chem. Soc., Faraday Trans. **89**, 1945 (1993).
[4] V. Meunier, Ph. Lambin, and A. A. Lucas, Phys. Rev. B **57**, 14 886 (1998).
[5] A. Bachtold, C. Strunk, J. Salvetat, J. Bonard, L. Forró, T. Nussbaumer, and C. Schönenberger, Nature (London) **397**, 673 (1999).
[6] J. O. Lee, J. R. Kim, J. J. Kim, J. Kim, J. W. Park, K. H. Yoo, and K. H. Park, Phys. Rev. B **61**, 16 362 (2000).
[7] H. Ajiki and T. Ando, J. Phys. Soc. Jpn. **65**, 505 (1996).
[8] S. Roche, G. Dresselhaus, M. S. Dresselhaus, and R. Saito, Phys. Rev. B **62**, 16 092 (2000); S. Roche and R. Saito, Phys. Rev. Lett. **87**, 246803 (2001).
[9] R. C. Haddon, Nature (London) **388**, 31 (1997).
[10] M. S. Ferreira, T. G. Dargam, R. B. Muniz, and A. Latgé, Phys. Rev. B **62**, 16 040 (2000).
[11] M. S. Ferreira, T. G. Dargam, R. B. Muniz, and A. Latgé, Phys. Rev. B **63**, 245111 (2001).
[12] C. G. Rocha, T. G. Dargam, and A. Latgé, Phys. Rev. B **65**, 165431 (2002).
[13] A. Latgé, D. C. Marcucci, and M. V. Tovar Costa, Physica E (Amsterdam) **13**, 12624 (2002).
[14] R. Saito, G. Dresselhaus, and M. S. Dresselhaus, *Physical Properties of Carbon Nanotubes* (Imperial College Press, London, 1998).
[15] G. W. Ho, A. T. S. Wee, and J. Lin, Appl. Phys. Lett. **79**, 260 (2001).
[16] M. F. Lin, R. B. Chen, and F. L. Shyu, Solid State Commun. **107**, 227 (1998).
[17] M. F. Lin and D. S. Chuu, Phys. Rev. B **57**, 6731 (1998).
[18] M. F. Lin, J. Phys. Soc. Jpn. **67**, 1094 (1998).
[19] J. W. Mintmire, B. I. Dunlap, and C. T. White, Phys. Rev. Lett. **68**, 631 (1992).
[20] N. Hamada, S. Sawada, and A. Oshiyama, Phys. Rev. Lett. **68**, 1579 (1992).
[21] D. Orlikowski, H. Mehrez, J. Taylor, H. Guo, J. Wang, and Christopher Roland, Phys. Rev. B **63**, 155412 (2001).
[22] M. Hjort and S. Stafström, Phys. Rev. B **61**, 14 089 (2000).
[23] T. Ando, T. Nakanishi, and M. Igami, J. Phys. Soc. Jpn. **12**, 3994 (1999).
[24] Hyoung J. Choi, J. Ihm, S. G. Louie, and M. L. Cohen, Phys. Rev. Lett. **84**, 2917 (2000).
[25] J. M. Luttinger, Phys. Rev. **84**, 814 (1951).
[26] H.-F. Cheung, Y. Gefen, E. K. Riedel, and W.-H. Shih, Phys. Rev. B **37**, 6050 (1988).
[27] Z. Barticevic, G. Fuster, and M. Pacheco, Phys. Rev. B **65**, 193307 (2002).
[28] C. L. Cheung, A. Kurtz, H. Park, and C. Lieber, J. Phys. Chem. **106**, 2429 (2002).
[29] Y. Kim and K. Chang, Phys. Rev. B **64**, 153404 (2001).
[30] H. Watanable, C. Manabe, T. Shigematsu, and M. Shimizu, Appl. Phys. Lett. **68**, 2928 (2001).